CFD Letters

Journal homepage:
https://semarakilmu.com.my/journals/index.php/CFD_Letters/index
ISSN: 2180-1363

Numerical and Experimental Validation of a New Methodology for the Design of Michel-Banki Turbine

Steven Galvis-Holguin[1,*], J. Sierra-Del Rio[2], Diana I. González-Arango[3], Edwin Correa-Quintana[3], Lisandra Da Rocha Meneses[4]

[1] Department of Mechatronics, Faculty of Engineering, Escuela Colombiana de Carreras Industriales, Medellín, Colombia
[2] Department of Mechanics Engineering, Faculty of Engineering, Institución Universitaria Pascual Bravo, research group GIIAN, Medellín, Colombia
[3] Department of Mechatronics and Electromechanics, Faculty of Engineering, Instituto Tecnológico Metropolitano, Medellín, Colombia
[4] Department of Applied Bioeconomy, Wrocław University of Environmental and Life Sciences, research group WBVG, Wrocław, Poland

ARTICLE INFO

Article history:
Received 22 April 2024
Received in revised form 20 May 2024
Accepted 19 June 2024
Available online 30 November 2024

Keywords:
Michell-Banki turbines; CFD; crossflow; renewable energy; experimental tests

ABSTRACT

Michell-Banki cross-flow turbines (MBT) are low-cost turbines that are easy to manufacture and maintain, which makes them ideal for implementation in small-scale hydroelectric projects. Although the MBT has lower efficiencies than turbines such as the Pelton and Francis, it maintains its efficiency stable in the face of fluctuations in flow conditions. The objective of this study is to validate, both numerically and experimentally, a new design methodology that allows the construction of an MBT based on site conditions. For this purpose, the design of the different components of an MBT was implemented according to the site conditions. The experimentation was carried out in a hydraulic test bench, which consists of a water tank, a $10\ HP$ centrifugal pump, a piping system, a PMAG SGM LEKTRA magnetic flow meter, a TRS605 FUTEK torque sensor, a pressure gauge, and a model of MBT designed and manufactured from scratch. It was concluded that the proposed methodology allows for obtaining experimental and numerical efficiencies of $72.9\ \%$ and $83.3\ \%$, respectively. Thus, a numerical-experimental validation of the MBT design and manufacturing methodology could be carried out.

1. Introduction

Sustainable development is currently of interest to researchers, due to the rapid growth in the level of greenhouse gas emissions and the rising cost of fuel [1]. Therefore, hydropower generation presents an efficient solution to achieve the right connection between renewable energy and sustainable development [2-4]. Given the above, it is now recognized as one of the most important forms of clean energy generation in the world, especially through Small Hydroelectric Power Plants (SHP's), which can be implemented in Non-Interconnected Zones (NIZs) in developing countries [5, 6]. Because electrification from interconnected systems is economically unfeasible.

* *Corresponding author.*
E-mail address: sgalvish@ecci.edu.co (Steven Galvis Holguin)

https://doi.org/10.37934/cfdl.17.5.7689

The Michell-Banki cross-flow turbine -MBT- is possibly the turbine with the greatest simplicity of design and construction [7, 8]. For this reason, they are among the low-cost HCP technologies, being widely used in some Asian countries such as Nepal [9]. MBT can be used in a wide range of flow rates and hydraulic head. However, they have a lower hydraulic efficiency compared to other turbines used in hydroelectric power plants such as the Francis, Pelton, and Kaplan [10]. As proposed by Prof. Banki, the original MBT had a theoretical efficiency of $87.8\ \%$, however, in constructing and testing the turbine, Mockmore and Merryfield obtained an efficiency of $68\ \%$ [11]. Since then, several numerical and experimental studies have been carried out, which are described below.

In the following, numerical investigations are presented in which the authors perform various geometrical modifications on the MBT rotor to improve its hydraulic performance: to exemplify, Bhagat *et al.,* [12] investigated by CFD, the effects of blade number, blade length, blade angle, rotor diameter, rotor height, and free-stream velocity on the performance of a cross-flow turbine rotor. Given this, with several 27 blades, an angle of $75\ °$, and a length of $30\ mm$ for the rotor design configuration, achieved significant power and efficient operation under free-flow conditions by achieving a reported maximum power/efficiency ratio of 0.389. In the same way, Jiyun *et al.,* [13] conducted a numerical investigation to study the effects of the outer rotor blade angle on turbine performance. The results with an angle of $30\ °$ indicated that the match between the flow inlet angle and the outer blade angle improved the torque output of the first rotor stage and the maximum turbine efficiency increased significantly from $45.9\ \%$ to $49.6\ \%$. In addition, Prabowoputra *et al.,* [14] studied the effect of increasing the number of rotor blades and blade angle on the performance of the MBT. This study was carried out using CFD, where the five-blade angles of attack, viz, $10\ ^{\circ}$, $15\ ^{\circ}$, $20\ ^{\circ}$, $25\ ^{\circ}$, and $30\ ^{\circ}$, were used to create variations. In addition to the number of blades with 12, 16, 20, 24, 32, 36, 40, 48 and 52. The results indicated that rotors with an angle of attack of $15\ °$ and several 40 blades performed better as they presented a maximum power coefficient of 0.327 at a rotational speed of $250\ rpm$. On the other side, apart from performance improvements with geometrical changes in the rotor, efficiency gains can also be realized by making geometrical changes to the injector. As in the case of Mehr *et al.,* [15] who designed the injector geometry and improved the performance of the MBT by analyzing various loading conditions. This turbine was designed using successive numerical simulations, and achieved a maximum hydraulic efficiency of $91\ \%$ and a maximum overall efficiency of $82\ \%$. On the other side, Ranjan *et al.,* [16] increased the performance of the MBT by changing the angle of the inlet arc of the injector from $65\ °$ to $85\ °$. In addition, they varied the rotational speed of the turbine from $200\ rpm$ to $800\ rpm$. With the above, they found that the maximum efficiency is of $97.8\ \%$ at an angle of the inlet arc of the injector of the $65\ °$ with a rotational speed of $600\ rpm$.

Concerning experimental investigations, the following authors performed geometrical modifications and validations of numerical methods of the MBT. For example, Leguizamón *et al.,* [17] investigated the trade-offs encountered during the design of these turbines, considering the limitations imposed by the available dimensions of commercial steel pipes. They introduced a computational model, evaluated its convergence, and validated it using experimental data. The case study revealed considerable efficiency, achieving a $75\ \%$. Subsequently, Bhagat *et al.,* [18] evaluated the performance of the cross-flow turbine for various design parameters, with different tip speeds (TSR), both numerically and experimentally. It was observed that the design parameters played a crucial role in improving rotor performance and auto-start capabilities. The parameters defined to evaluate the turbine performance were the maximum torque and power coefficient, which were 1.08 and 0.267, respectively. Finally, in terms of experimental research, Capera *et al.,* [19] designed and numerically evaluated an MBT for specific flow conditions of $0.24\ \frac{m^3}{s}$ and a height of $18\ m$, corresponding to an operating point. Both the experimental design and simulation results indicate that the design is feasible for the operating conditions and meets the performance expectations for a micro-hydroelectric power plant installation. An unusually high efficiency was predicted from the $86.3\ \%$ in the design, whereas the simulation reported an efficiency of $51.8\ \%$. For an average of $78\ \%$.

Based on the state of the art, it was determined that most of the experimental studies performed to increase the efficiency of MBT have focused on specific geometrical parameters, which have reported different maximum efficiency values. Although the results may have depended on the resolution of the instrumentation used and the laboratory setup, the results indicate that there is still potential for improvement in MBT. However, none has experimentally validated a complete design methodology, which aids in the sizing of each of the MBT components according to site conditions. Because of this, the objective of this study is to validate both numerically and experimentally a new design methodology for MBT, via computational simulations and hydraulic bench tests, in which the design of the different components of an MBT according to site conditions is implemented.

2. Methodology

MBT consists of an injector, a rotor, and a casing. The rotor consists of two parallel discs joined together by several blades. The injector, consisting of a rectangular section at the beginning, directs the water flow to the impeller, which hits the blades at the outlet of the injector and flows through the channels between the blades for the first time. It then passes through the space in the center of the impeller and finally, it passes through the blades a second time, leaving the impeller in a radial direction [11, 20]. Finally, the housing does not influence the efficiency of the MBT, however, it varies according to the installation conditions of the turbine. Considering the above, the MBT is a turbomachine that transfers energy between the fluid and the blades in two stages (Figure 1), transferring $75\ \%$ and $25\ \%$ of the energy in the first and second stages, respectively [21]. This flow phenomenon has led to the MBT being considered a two-stage partial impulse turbine, because the first stage operates on the reaction grade and the second stage operates on the pure impulse principle [11, 20].

The methodology of this work will be divided into three phases: design and governmental equations, numerical simulations, and experimental tests. To contrast the numerical-experimental results of the designed MBT working under the same nominal design conditions (flow and head).

2.1 Numerical Model

The theoretical approach described by Sammartano *et al.,* [22] shows that the maximum efficiency is obtained when the tangential velocity of the particle is approximately twice the tangential velocity of the system, as shown in Eq. (1):

$$v \cos \alpha = 2\omega R_1 \tag{1}$$

Where v is the absolute speed at rotor entry, α is the angle of attack, ω is the rotational speed of the rotor, and R_1 is the outer radius of the rotor, as shown in Figure 1. Then, Eq. (2) is given, which determines the Torricelli efficiency ratio between the rotor input speed and the net head (H) at the turbine inlet. Where C_v is the coefficient of velocity loss, assumed as 0.98, as the inlet is at atmospheric pressure [23]. On the other part, g refers to the acceleration of gravity, with a value of $9.81\ \frac{m}{s^2}$.

$$v = C_v\sqrt{2gH} \tag{2}$$

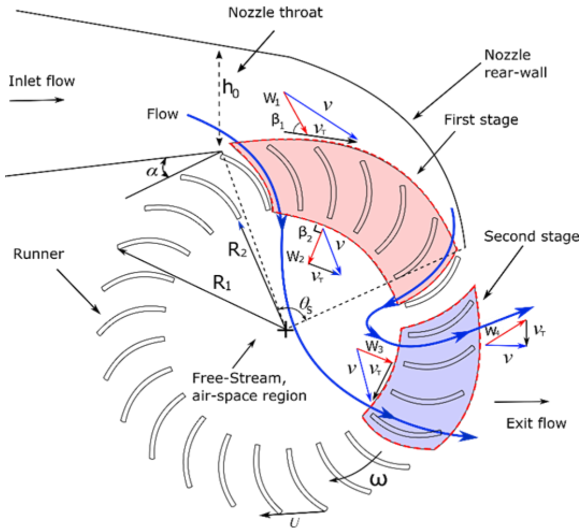

Fig. 1. Geometrical scheme of the MBT and the particle in motion within the rotating reference frame. Source: Adapted from [9]

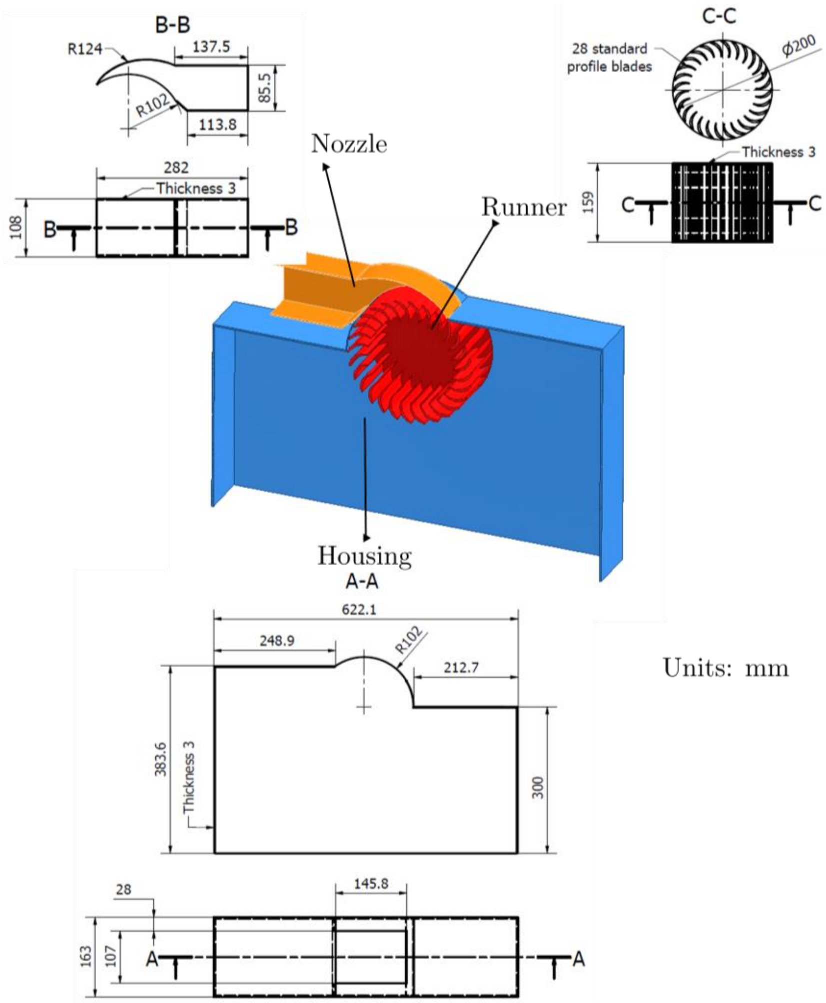

Fig. 2. Isometric view of the CAD model of the designed MBT, with the structural dimensions of each element

This work allowed the continuation of the work carried out by Galvis-Holguín *et al.,* [24] who designed in detail the MBT model used in this study, starting from the flow conditions (flow and head) and based on Eq. (1) and Eq. (2). Taking this into account, the simplified CAD design of the elements (rotor, injector, and casing) that constitute the MBT is presented, as shown in Figure 2.

A Boolean operation was then performed to obtain the internal control volume, which is discretized in the Mesh module of the Ansys 2022 R3® software, using tetrahedral elements with advanced curvature and proximity functions, with a minimum element size of $2\ mm$, which was sufficient to determine mesh independence.

Subsequently, for the configuration of the CFD simulation, different investigations were taken into account where the different turbulence models are compared in turbo-machinery problems using the CFX module of the Ansys® program and in some different computational models. The turbulence model $k-\varepsilon$ standard correctly describes the flow in different numerical models with problems similar to that of turbo-machinery, and adequately characterizes the flow inside the cross-flow turbine [25]**.** This turbulence model combines numerical robustness and reduced computational cost compared to other turbulence models such as SST $k-\omega$, providing a reasonable accuracy not only for the current problem [26, 27]. Therefore, the turbulence model was used in this work $k-\varepsilon$ standard, for a time-dependent analysis, based on transient simulations, which had a total simulation time of $1\ s$ and a time step of $0.001\ s$. In addition, the homogeneous two-phase model composed of water and air was considered to determine the interaction of both fluids inside the turbine. The homogeneous free surface model allows creating of a coupling between the two phases where they share the same dynamic fields of pressure, velocity, and turbulence [27]**.** In addition, a standard fluid temperature for this type of hydraulic turbines is taken into account equal to $25\ °C$.

It is important to note that the models that have been widely used by most researchers for two-phase models are the homogeneous model and the separated flow model. The latter is a simple version of the multi-fluid model; it allows two phases to have different one-dimensional properties and velocities, while the conservation equations are written for the combined flow. On the other hand, the homogeneous flow model provides a simpler approach to determine flow properties and behaviors, but underestimates pressure drops. In addition, it is less accurate when the velocity and flow conditions for both phases are dispersed. On the other hand, a separate flow model is more robust and better predicts behavior in multiphase simulations with more accurate results, but at a higher computational cost [28]**.**

2.2 Experimental Model

The experimental model was used to examine the characteristic performance and to validate a design methodology based on the site conditions for an MBT, in which the same dimensions were used in both the numerical and experimental stages. The installation consists of a model MBT, a water tank, a $10\ HP$ centrifugal pump, a piping system, a PMAG SGM LEKTRA magnetic flow meter, a TRS605 FUTEK torque sensor and a pressure gauge at the MBT inlet.

Water from the reservoir was pumped to the MBT while the flow rate measured by the flow sensor was regulated by controlling the pump frequency using a variable speed drive. Simultaneously, the pressure at the turbine inlet was measured by the pressure gauge, and obtaining the torque and angular velocity at the turbine shaft was performed by the torque sensor. The experimental setup is detailed in the schematic in Figure 3.

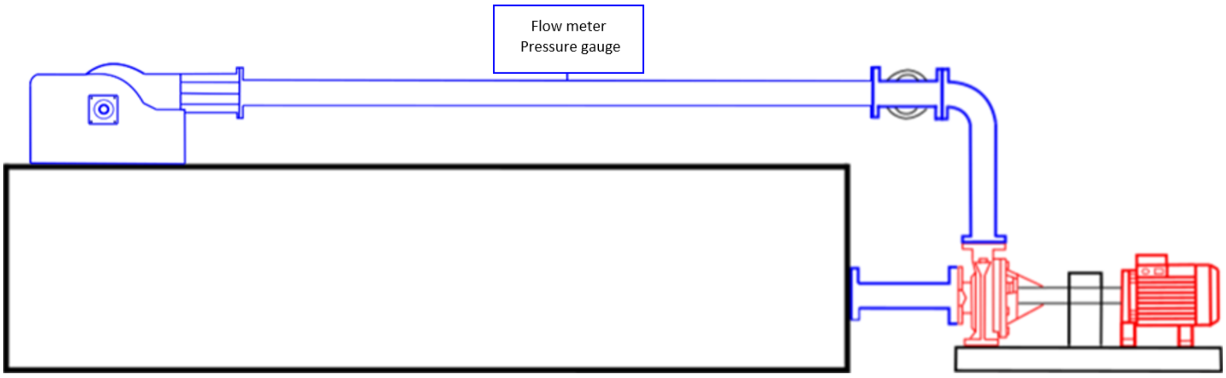

Fig. 3. Diagram of the hydraulic bench

After having the configuration of the experimental bench, the system that serves as a brake for the torque sensor must be manufactured, since it works utilizing a set of strain gauges with a Wheatstone bridge configuration inside, which yields a voltage differential to torsional deformations. Therefore, a system is needed that is directly coupled to the sensor shaft, while the latter is simultaneously coupled to the turbine shaft, as shown in Figure 4. In this case, the motor will function as a brake by providing a torsional force to the sensor in the opposite direction of the turbine rotor. Providing the torque, angular velocity, and power generated by the turbine. In addition, a flexible coupling must be used for the sensor and turbine coupling, to avoid vibrations that may occur in the operation of the turbine and thus reduce noise in the torque measurement. Then, the counter torque system is coupled to the turbine using a spider coupling, ensuring concentricity between shafts employing levelers.

Fig. 4. Experimental setup of the MBT

3. Results

3.1 Numerical Results

In this section we will first analyze the results of the numerical model implemented and then the experimental validation of the model. Figure 5 shows the efficiency based on the number of elements for the studied model. For the mesh independence study of the MBT, five different meshes starting from 2.1 to 10.3 million elements were applied. In the numerical computation as the mesh cell size decreases, the results obtained in the CFX solver are more accurate. However, the computational cost is higher. In this way, it was determined that the error rate of mesh three with respect to mesh four was 1.5 %. On the other hand, the error rate of mesh four with respect to mesh five was 0.8 %, below the convergence criterion taken into account in this study 1 %. Therefore, mesh four was selected because it meets the convergence criterion defined in this study, guaranteeing a more accurate result compared to mesh three and a lower computational cost compared to mesh five. This result was obtained following the methodology of the study carried out by Hang *et al.,* [29].

Additionally, constant monitoring of the torque generated by the turbine as a function of time was carried out, allowing to guarantee the stability of the response both numerically for RMS below $1E-4$, and at the steady flow condition level by showing that the torque does not vary as a function of turbine rotation, reaching stationary operating conditions [30].

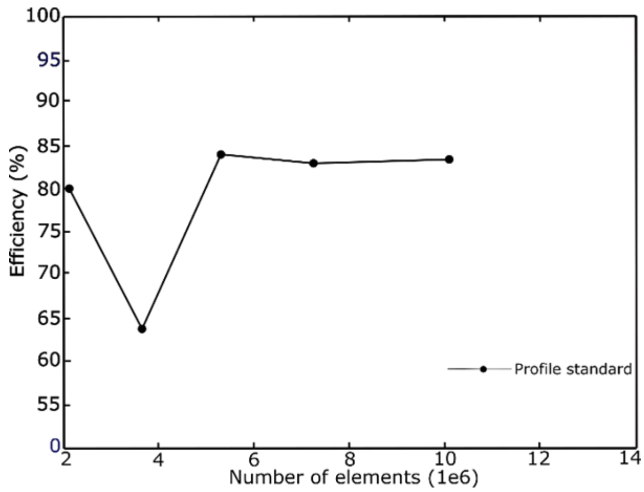

Fig. 5. Mesh independence for the model under study

Figure 6 shows the volume fraction contour in the symmetry plane (XY) of the MBT, where the red color with a value of 1 represents the water and the blue color with a value of 0 represents the air inside the MBT. It can be seen the passage of water from the injector and then through the rotor, creating the so-called cross-flow between the first and second stages of energy delivery.

In addition, it is possible to observe no flow separation when passing from the first to the second stage of the MBT. This may be due to the correct design of the back wall of the injector proposed by Adhikari *et al.,* [9] which allows a better match between the angles of the relative fluid velocity and the position of the blades ($\beta_1 \approx \beta_{1b}$), along the azimuthal position at the inlet of the first rotor stage.

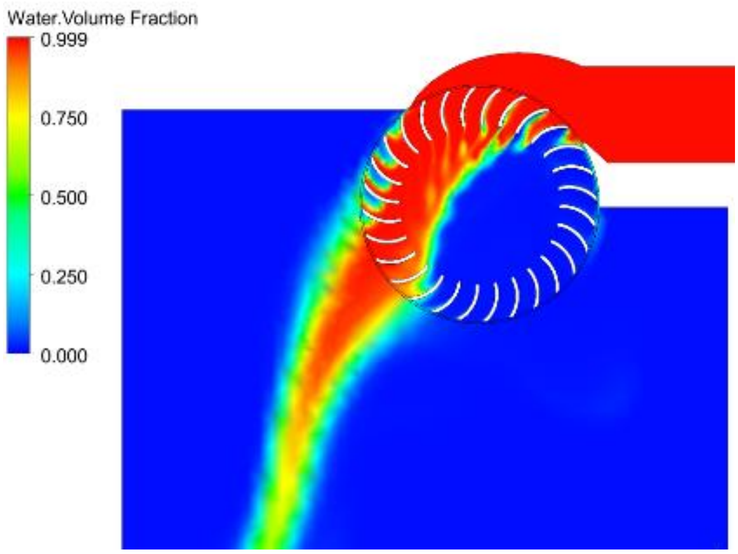

Fig. 6. Water volume fraction contour in the turbine symmetry plane

Figure 7 shows the pressure contour in the (XY) plane of symmetry through the injector and the rotor of the MBT. In this graphical representation, it is possible to observe areas of negative pressures on the convex faces of the blades, which allows the MBT to operate as a reaction turbine in the first stage, allowing to increase in the turbine power output, due to the lift force created by the pressure differences in the rotor blades. The above confirms the statement made by Mockmore and Sammartano *et al.,* [11, 20].

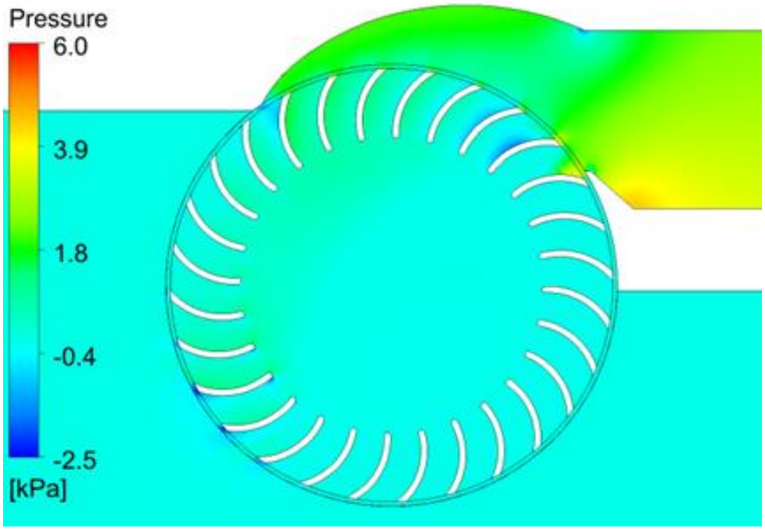

Fig. 7. Total pressure contour in the symmetry plane of the MBT

In Figure 8, the velocity vectors in the (XY) plane of symmetry through the injector and the rotor of the MBT are presented. One can observe an increase in fluid velocity through the injector and then a deceleration of the fluid as it enters the first stage of the rotor. This is because the fluid delivers most of its kinetic energy to the blades of the MBT. In addition, it is observed that between the convex and concave part of the blades there is a velocity differential, causing low-pressure zones to be generated where the lowest velocities are between the blade faces. This explains why there are negative pressures on the convex faces of the blades.

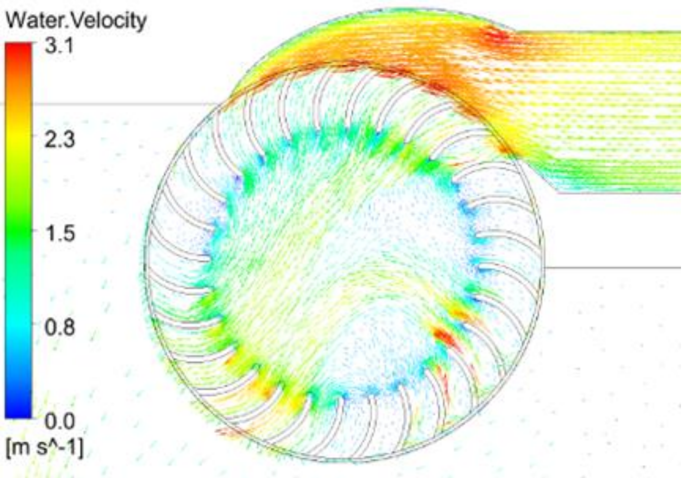

Fig. 8. Velocity vectors in the symmetry plane of the MBT

Finally, regarding the numerical model, the characterization of the MBT was performed to verify the behavior of the efficiency with changes in the rotational speed, for which the efficiency was plotted against the speed ratio (V_t/U). The latter is a dimensionless number that relates the tangential fluid velocity (V_t) and rotor (U). Allowing to characterize the operating conditions of hydraulic and wind turbines, which determines the operating range of each class of turbine.

Figure 9 shows the efficiency of the MBT for different rotational speeds of the turbine. The curve highlighted in red corresponds to the numerical results of the current study, for which six simulations were performed by varying the angular velocity from 100 to $200\ RPM$, with steps of $20\ RPM$. Obtaining the highest performance for a speed of $160\ RPM$ with a numerical efficiency of $83.3\ \%$. On the other hand, the curve highlighted in blue and the black triangles correspond to the numerical and experimental results obtained by Sammartano *et al.,* [31] respectively.

Based on the foregoing, this study showed similarities with the numerical-experimental study conducted by Sammartano *et al.,* [31] in which they obtained maximum efficiencies of $83.1\ \%$ and $77.4\ \%$, for numerical simulations and experimental tests, respectively. In addition, both studies presented their highest efficiency for velocity ratios close to 1.7.

The result of this work could be validated by different literature works, which found the maximum efficiency of MBT for speed ratios between 1.7 and 2.0 [27, 32]. With this ratio, it is possible to establish the energy extraction capacity as a function of the speed ratio, which is conditioned to the rotational speed of the turbine. With this, it is sought to determine the ideal rotation speed to commercially select a power transmission system for the commercial electric generator.

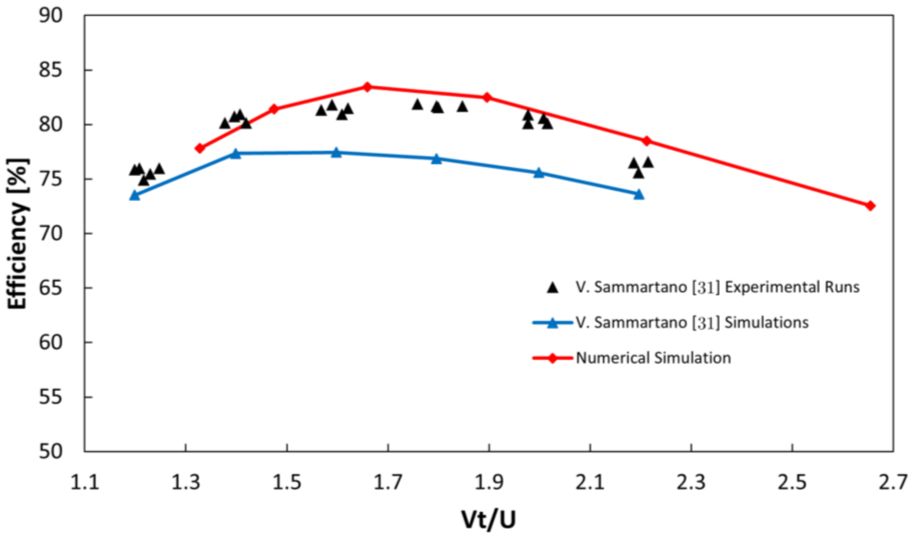

Fig. 9. Efficiency of MBT as a function of the speed ratio obtained for the present study and by the research by V. Sammartano [31]

From the results obtained and discussed above, it could be evidenced that the MBT obtained a correct hydrodynamic performance in the CFD tests, reaching numerical efficiencies of up to $83.3\ \%$. For this reason, the construction and experimental tests of the scale model are carried out on the hydraulic bench. To validate the numerical results presented.

3.2 Experimental Results

Figure 10 shows the efficiency curves of the MBT, both for the numerical simulations represented by the green curve and for the experimental tests represented by the orange curve, corresponding to a flow of $16.2\,\frac{l}{s}$, in both cases. The experimental curves were obtained as follows: the flow rate was measured using a LEKTRA brand PMAG SGM non-invasive magnetic flow sensor, the static pressure was obtained using an analog pressure gauge at the inlet of the MBT injector and the dynamic pressure was theoretically calculated using Bernoulli's principle. In addition, the hydraulic power output was measured using the TRS605 torque sensor and the IHH500 Elite display, both FUTEK brand.

It was possible to verify that the maximum efficiency of the MBT for conditions below the design speed ratio is greater than 1.7, Consequently, when the operating flow rate decreases, the optimum rotor rotational speed decreases. However, the efficiency is not considerably affected. On the other hand, it can be evidenced that the numerical curve and the experimental curve with the same operating flow rate present the highest efficiency at the same speed ratio, equal to 1.7. This indicates that, as the flow rate entering the MBT increases, the optimum rotational speed increases.

Concerning the maximum efficiencies determined, it was possible to find a numerical and experimental efficiency of 83.3 % and 72.9 %, respectively. In addition, it was observed that the turbine maintained its efficiency above 55 % due to changes in the rotational speed. Therefore, it can be corroborated that MBTs allow having relatively stable efficiencies in the face of changes in the operating conditions, compared to other turbines such as the Pelton and Francis. In addition, the numerical and experimental efficiency curves are compared from the calculation of the relative error for the points with a speed ratio equal to 1.7, reporting an error of 12.4 % at the point of highest efficiency.

The authors report this result as a relatively high error. However, this error was attributed to the manufacturing processes established for the experimental model that could not be taken into account in the simulations. The error between experimentation and simulations is attributed to four reasons: The first, is due to the unbalance in the rotor, which can produce mechanical losses in the bearings and the whole coupling system. Second, the simulations did not take into account the roughness of the MBT manufacturing materials. Third, the losses after the pressure gauge were not accounted for and fourth, the roughness of the materials used in the manufacturing process was not configured in the numerical simulations. Due to this, the authors consider that this error is acceptable to validate the numerical method used in this study.

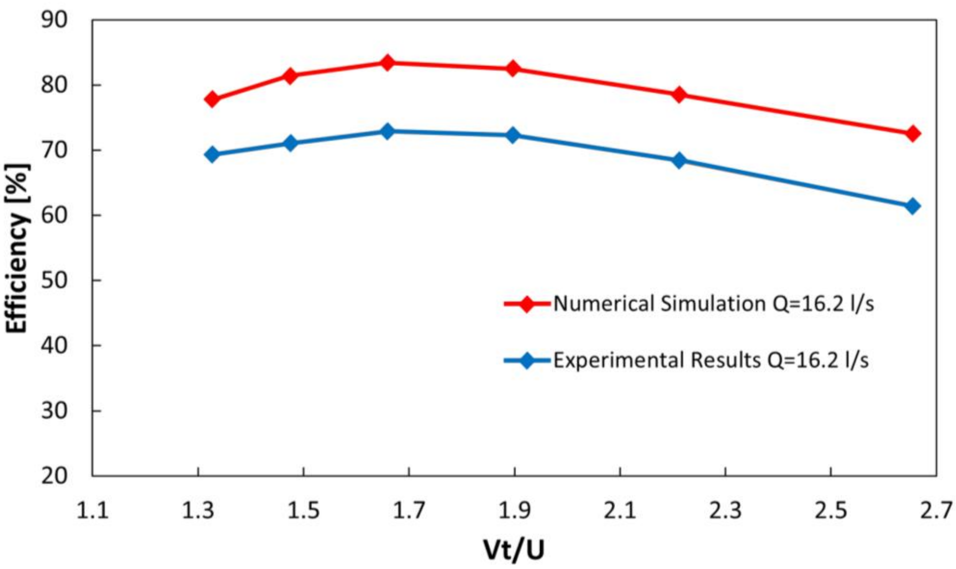

Fig. 10. Experimental and numerical curves of efficiency vs. speed for different flow conditions

It can be observed that, despite having an error of $12.4\ \%$ between the experimental and numerical simulations, the tendency to maintain the efficiency in a higher RPM range as the flow conditions increase is also maintained for the numerical simulations. Additionally, it can be evidenced that for both the experimental and numerical curves, operating under the same flow and head conditions, a similar tendency is presented in the face of variations in the rotation conditions.

For future simulations on this experimental model, the computational model will be adjusted with the roughness of the material established for manufacturing, in addition to the turbulence at the inlet of the system. On the other hand, the structural corrections of the experimental model will have to be made, such as the unbalance in the rotor, the quality of the bearings, the surface finish of the blades, and the accounting of the error of the measuring instruments.

Additionally, to demonstrate the novelty of this study, a literature comparison was performed in terms of the different geometric parameters that have been studied about MBT design. Table 1 presents the numerical values of the design parameters, including the flow rate Q, head H, injector width B, rotor width W, injector height at discharge h_o, outer diameter of the rotor D_1, inner diameter D_2, injector opening θ_s, the angle of the velocity relative to the input β_1, the angle of the velocity relative to the output β_2, angle of attack α_1, the angular velocity of the rotor ω, blade thickness e, number of blades N_b, power generated P_t and finally, the efficiency n.

The above showed that this study presented a correct hydrodynamic performance in comparison with the studies reported in the literature. This allowed to experimentally validate a modified design methodology proposed by the study of Galvis-Holguín *et al.,* [24] for MBT, finding similar results with other design methodologies both numerically and experimentally, which were reported in Table 1.

Table 1
Comparison of geometric parameters related to MBT design as reported in the literature and the present study

	Operation condition		***Parameter Nozzle***			***Parameter Runner***									***Results***	
Symbol Units	$\boldsymbol{Q}$ $\left[\frac{\mathrm{m}^3}{\mathrm{s}}\right]$	$\mathbf{H}$ $[\mathrm{m}]$	$\mathbf{B}$ $[\mathrm{m}]$	$\boldsymbol{h_0}$ $[\mathrm{m}]$	$\boldsymbol{\theta_s}$ $[°]$	$\boldsymbol{D_1}$ $[\mathrm{m}]$	$\boldsymbol{D_2}$ $[\mathrm{m}]$	$\mathbf{W}$ $[\mathrm{m}]$	$\boldsymbol{\beta_1}$ $[°]$	$\boldsymbol{\beta_2}$ $[°]$	$\boldsymbol{\alpha_1}$ $[°]$	$\boldsymbol{\omega}$ $[\mathrm{RPM}]$	$\boldsymbol{e}$ $[\mathrm{m}]$	$\boldsymbol{N_b}$ $[-]$	$\boldsymbol{P_t}$ $[\mathrm{kW}]$	$\boldsymbol{n}$ $[\%]$
Actual	0.016	0.5	0.103	0.065	90	0.200	0.136	0.155	36	90	20	160	3.0	28	0.06	83.3
[9]	0.046	1.3	0.102	0.089	90	0.305	0.207	0.102	39	90	22	199	3.2	30	0.53	88.8
[26]	-	5	-	-	90	-	-	-	30	90	16	350	-	24	-	79.0
[33]	-	5	0.190	0.065	120	0.135	0.095	0.190	26	90	12	350	-	24	-	89.0
[32]	0.060	10	0.093	0.047	90	0.161	0.109	0.139	39	90	22	757	-	35	5.20	88.4
[34]	0.040	2.7	0.106	0.053	112	0.180	0.117	0.159	42	90	22	390	-	25	-	55.3
[35]	0.060	17	0.083	0.047	90	0.161	0.104	0.139	39	90	22	-	-	35	7.76	77.8
[36]	0.100	10	-	-	-	0.200	0.136	-	-	90	7	642	-	22	7.21	76.6
[37]	0.105	10	0.094	0.083	80	0.316	0.212	0.094	39	90	22	500	3.0	35	7.00	91.0

4. Conclusions

This work presents the experimental validation of a numerical methodology previously used for the design of an MBT. This uses the scale construction and commissioning of the designed model on a hydraulic test bench. The conclusions obtained for this study are summarized below:

The numerical methodology implemented for the turbine in this study was experimentally validated, achieving a numerical and experimental hydraulic performance of $83.3\ \%$ and $72.9\ \%$, respectively. Obtaining an error of $12.4\ \%$ between the two stages, which is attributed to the following reasons: The first, is mechanical losses due to unbalance in the MBT rotor. Second, the simulations did not take into account the exact roughness of the walls, the losses of the measuring instruments, the friction losses in the bearings, and the error of the instruments.

Finally, a functional prototype of the turbine was obtained using affordable and low-cost prototyping methodologies, thus guaranteeing the implementation of this technology in areas with low technical and economic resources.

Acknowledgement
This research was carried out thanks to the computer equipment available at the Instituto Tecnológico Metropolitano used for CFD simulation, and to the experimental test bench of the Universidad de Antioquia.

References

[1] Algarni, Salem, Vineet Tirth, Talal Alqahtani, Sultan Alshehery, and Pravin Kshirsagar. "Contribution of renewable energy sources to the environmental impacts and economic benefits for sustainable development." *Sustainable Energy Technologies and Assessments* 56 (2023): 103098. https://doi.org/10.1016/j.seta.2023.103098
[2] Adanta, Dendy, and Ahmad Indra Siswantara. "Assessment of turbulence modelling for numerical simulations into pico hydro turbine." *Journal of Advanced Research in Fluid Mechanics and Thermal Sciences* 46, no. 1 (2018): 21-31.
[3] Basar, Mohd Farriz, Nurul Ashikin M. Rais, Azhan Ab Rahman, Wan Azani Mustafa, Kamaruzzaman Sopian, and Kaifui V. Wong. "Optimization of reaction typed water turbine in very low head water resources for Pico Hydro." *Journal of Advanced Research in Fluid Mechanics and Thermal Sciences* 90, no. 1 (2022): 23-39. https://doi.org/10.37934/arfmts.90.1.2339
[4] Suarda, Made, Made Sucipta, and Ibnu Gusti Muttakin. "Semi twisted curve blade vortex turbine performance at runner rotation speed variation using CFD simulation." *Journal of Advanced Research in Fluid Mechanics and Thermal Sciences* 104, no. 2 (2023): 26-35. https://doi.org/10.37934/arfmts.104.2.2635
[5] Temel, Pelin, Elcin Kentel, and Emre Alp. "Development of a site selection methodology for run-of-river hydroelectric power plants within the water-energy-ecosystem nexus." *Science of the Total Environment* 856 (2023): 159152. https://doi.org/10.1016/j.scitotenv.2022.159152
[6] Rodas, Carlos Artemio Macias, Pascual Lopez de Paz, Orlando Lastres Danguillecourt, and Guillermo Ibáñez Duharte. "Analysis and optimization to a test bench for Micro-hydro-generation." *Energy Reports* 8 (2022): 321-328. https://doi.org/10.1016/j.egyr.2022.10.292
[7] Mereke, Nebiyu Bogale, Venkata Ramayya Ancha, and Patrick Hendrick. "Numerical modeling and CFD simulation of diffuser augmented dual vertical axis hydrokinetic Banki-Michell turbine." *Heliyon* 10, no. 5 (2024). https://doi.org/10.1016/j.heliyon.2024.e26970
[8] Dragomirescu, Andrei, and Mihai Schiaua. "Experimental and numerical investigation of a Bánki turbine operating far away from design point." *Energy Procedia* 112 (2017): 43-50. https://doi.org/10.1016/j.egypro.2017.03.1057
[9] Adhikari, R. C., and D. H. Wood. "A new nozzle design methodology for high efficiency crossflow hydro turbines." *Energy for Sustainable Development* 41 (2017): 139-148. https://doi.org/10.1016/j.esd.2017.09.004
[10] Ha, Hojin, Sangwoo Ham, EHSAN ADEEB, and Jeong Wan Lee. "Numerical Evaluation of Low-Head Inverted Cross-Flow Turbine Design Methodology: A Comprehensive Study." *Available at SSRN 4479475*.
[11] C. A. Mockmore and F. Merryfield, *THE BANKI WATER TURBINE*, Bulletin Series 25. Oregon State College, 1949. Accessed: Jun. 26, 2024.
[12] Bhagat, Ravindra, Dinesh Kumar, and Shibayan Sarkar. "Employability of vertical axis crossflow whirlybird rotor as hydrokinetic turbine and its performance prediction corresponding to different design parameters." *Ocean Engineering* 238 (2021): 109744. https://doi.org/10.1016/j.oceaneng.2021.109744
[13] Jiyun, Du, Shen Zhicheng, and Yang Hongxing. "Study on the effects of blades outer angle on the performance of inline cross-flow turbines." *Energy Procedia* 158 (2019): 1039-1045. https://doi.org/10.1016/j.egypro.2019.01.252
[14] Prabowoputra, Dandun Mahesa, Aditya Rio Prabowo, Indri Yaningsih, Dominicus Danardono Dwi Prija Tjahjana, Fajar Budi Laksono, Ristiyanto Adiputra, and Hendri Suryanto. "Effect of Blade Angle and Number on the Performance of Bánki Hydro-Turbines: Assessment using CFD and FDA Approaches." (2023): 519-530. https://doi.org/10.5109/6782156
[15] Mehr, Goodarz, Mohammad Durali, Mohammad Hadi Khakrand, and Hadi Hoghooghi. "A novel design and performance optimization methodology for hydraulic Cross-Flow turbines using successive numerical simulations." *Renewable Energy* 169 (2021): 1402-1421. https://doi.org/10.1016/j.renene.2021.01.090

[16] Ranjan, Rajeev Kumar, Nur Alom, Jaswant Singh, and Bikash Kumar Sarkar. "Performance investigations of cross flow hydro turbine with the variation of blade and nozzle entry arc angle." *Energy conversion and management* 182 (2019): 41-50. https://doi.org/10.1016/j.enconman.2018.12.075

[17] Leguizamón, Sebastián, and François Avellan. "Computational parametric analysis of the design of cross-flow turbines under constraints." *Renewable Energy* 159 (2020): 300-311. https://doi.org/10.1016/j.renene.2020.03.187

[18] Bhagat, Ravindra, Dinesh Kumar, and Shibayan Sarkar. "Design modification and performance prediction of ellipsoid cross-flow hydrokinetic turbine." *Renewable Energy* 219 (2023): 119475. https://doi.org/10.1016/j.renene.2023.119475

[19] Capera, Freddy Sotto, Juan Gonzalo Ardila Marín, and Camila Cerquera Sandoval. "Numerical Study of the Opening Angle Incidence in Michell-Banki Turbine's Performance without Guide Blades." *International Journal of Engineering Research in Africa* 67 (2023): 101-122. https://doi.org/10.4028/p-EO6We7

[20] Sammartano, Vincenzo, Gabriele Morreale, Marco Sinagra, and Tullio Tucciarelli. "Numerical and experimental investigation of a cross-flow water turbine." *Journal of Hydraulic Research* 54, no. 3 (2016): 321-331. https://doi.org/10.1080/00221686.2016.1147500

[21] D. G. Shepherd, *Principles of turbomachiney*, 17th ed. Technology & Engineering, 1956. Accessed: Jun. 26, 2024.

[22] Sammartano, Vincenzo, Costanza Aricò, Armando Carravetta, Oreste Fecarotta, and Tullio Tucciarelli. "Banki-Michell optimal design by computational fluid dynamics testing and hydrodynamic analysis." *Energies* 6, no. 5 (2013): 2362-2385. https://doi.org/10.3390/en6052362

[23] Quaranta, Emanuele, Jean Pierre Perrier, and Roberto Revelli. "Optimal design process of crossflow Banki turbines: Literature review and novel expeditious equations." *Ocean Engineering* 257 (2022): 111582. https://doi.org/10.1016/j.oceaneng.2022.111582

[24] Galvis-Holguin, Steven, Jorge Sierra-Del-Rio, Diego Hincapié-Zuluaga, and Edwin Chica-Arrieta. "Numerical validation of a design methodology for crossflow turbine type Michell-Banki." *Tecnología y Ciencias del Agua* 12, no. 5 (2021). https://doi.org/10.24850/j-tyca-2021-05-03

[25] Woldemariam, Endashaw Tesfaye, Hirpa G. Lemu, and G. Gary Wang. "CFD-driven valve shape optimization for performance improvement of a micro cross-flow turbine." *Energies* 11, no. 1 (2018): 248. https://doi.org/10.3390/en11010248

[26] Kaunda, Chiyembekezo S., Cuthbert Z. Kimambo, and Torbjorn K. Nielsen. "A numerical investigation of flow profile and performance of a low cost Crossflow turbine." *International Journal of Energy & Environment* 5, no. 3 (2014).

[27] Sammartano, Vincenzo, Gabriele Morreale, Marco Sinagra, and Tullio Tucciarelli. "Numerical and experimental investigation of a cross-flow water turbine." *Journal of Hydraulic Research* 54, no. 3 (2016): 321-331. https://doi.org/10.1080/00221686.2016.1147500

[28] Massoud, Mahmoud. "Two-Phase Flow and Heat Transfer." *Engineering Thermofluids: Thermodynamics, Fluid Mechanics, and Heat Transfer* (2005): 601-686.

[29] Hang, Leong Chee, Nur Athirah Nadwa Rosli, Mastura Ab Wahid, Norazila Othman, Shabudin Mat, and Mohd Zarhamdy Md Zain. "CFD Analysis on Propeller at Varying Propeller Disc Angle and Advance Ratio." *Journal of Advanced Research in Fluid Mechanics and Thermal Sciences* 96, no. 1 (2022): 82-95. https://doi.org/10.37934/arfmts.96.1.8295

[30] Ceballos, Y. Castañeda, M. Cardona Valencia, Diego Hincapie Zuluaga, J. Sierra Del Rio, and S. Vélez García. "Influence of the number of blades in the power generated by a Michell Banki Turbine." *International Journal Of Renewable Energy Research IJRER* 7, no. 4 (2017): 1989-1997.

[31] Sammartano, V., G. Morreale, M. Sinagra, A. Collura, and T. Tucciarelli. "Experimental study of cross-flow micro-turbines for aqueduct energy recovery." *Procedia Engineering* 89 (2014): 540-547. https://doi.org/10.1016/j.proeng.2014.11.476

[32] Sammartano, Vincenzo, Costanza Aricò, Armando Carravetta, Oreste Fecarotta, and Tullio Tucciarelli. "Banki-Michell optimal design by computational fluid dynamics testing and hydrodynamic analysis." *Energies* 6, no. 5 (2013): 2362-2385. https://doi.org/10.3390/en6052362

[33] Chichkhede, Shashi, Vinay Verma, Vivek Kumar Gaba, and Shubhankar Bhowmick. "A simulation based study of flow velocities across cross flow turbine at different nozzle openings." *Procedia Technology* 25 (2016): 974-981. https://doi.org/10.1016/j.protcy.2016.08.190

[34] Warjito, R. D., A. I. Siswantara, D. Adanta, A. P. Prakoso, and R. Dianofitra. "Comparison between Airfoil NACA-6712 Profiled and Ordinary Blade in Cross-flow Turbine by Numerical Simulation." In *The 15th International Conference on Quality in Research (QiR 2017). Available at: https://scholar. ui. ac. id/en/publications/comparison-between-airfoil-naca-6712-profiled-and-ordinary-blade*. 2017.

[35] Adanta, Dendy, and Aji Putro Prakoso. "Performance comparison of NACA 6509 and 6712 on pico hydro type cross-flow turbine by numerical method." *Journal of Advanced Research in Fluid Mechanics and Thermal Sciences* 45, no. 1 (2018): 116-127.
[36] Acharya, Nirmal, Chang-Gu Kim, Bhola Thapa, and Young-Ho Lee. "Numerical analysis and performance enhancement of a cross-flow hydro turbine." *Renewable energy* 80 (2015): 819-826. https://doi.org/10.1016/j.renene.2015.01.064
[37] Adhikari, Ram, and David Wood. "The design of high efficiency crossflow hydro turbines: A review and extension." *Energies* 11, no. 2 (2018): 267. https://doi.org/10.3390/en11020267